Proteome allocation influences population dynamics in microbial communities

Leonardo Pacciani-Mori,[1,2,*] Andrea Giometto,[2,3] Samir Suweis,[1] and Amos Maritan[1]

[1] *Department of Physics and Astronomy "Galileo Galilei", University of Padova, Via Marzolo 8 35131, Padova (Italy)*

[2] *Department of Physics, Harvard University 17 Oxford St, Cambridge 02138 MA*

[3] *Department of Molecular and Cellular Biology, Harvard University 52 Oxford St, Cambridge 02138 MA*

(Dated: December 30, 2019)

Microbial communities are complex systems, and the fundamental mechanisms that control their dynamics and composition are still largely unknown. Here we show that such systems have a previously unexplored level of complexity: their microscopic details related to gene expression influence their macroscopic properties such as the population dynamics. We provide an experimental proof of concept showing that proteome allocation dramatically affects the outcome of competition assays between strains of *Escherichia coli*. We also provide an essential model that predicts our findings.

Microbes are among the most abundant life forms on Earth [1]. They inhabit almost every habitat of our planet, and have continuously surprised us for their ability to survive in places that were thought to be inhospitable and barren. For example, microbial communities have been found in the deep terrestrial subsurface [2, 3], and it has been estimated that the first five kilometers beneath the Earth's surface could be habitable for them [4]. Because of their ubiquity, microbial communities play fundamental roles in countless natural processes of vital importance, from the digestion and overall health of their host organism [5] to climate regulation [6, 7]. Despite their importance, however, we still know very little about the fundamental mechanisms that regulate microbial communities, partly because we are only able to grow in the lab a very small fraction of all the bacteria found in nature [8], and partly because microbial communities are complex, non-linear systems whose dynamics is difficult to predict. Such difficulty arises because microbial communities are comprised of multiple agents (e.g., different species) linked by numerous kinds of interactions, and often the properties of the whole system cannot be inferred directly from the properties of its constituent parts alone. For these reasons, scientists from many disciplines have long been fascinated by the challenging theoretical questions posed by the study of microbial communities' structure and dynamics, and serious efforts have been made to understand how competition [9–11] and metabolic interactions [12, 13] allow such systems to maintain very high levels of biodiversity.

Recent studies have shown that the structure and composition of microbial communities are tightly linked to the metabolism of the species that comprise them [14, 15] (e.g., communities with different taxonomic composition can nevertheless exhibit the same metabolic functional structure [16, 17]). We can therefore speculate that the ways with which they consume different resources for growth and proliferation can affect the dynamics of the entire community. On the other end, nutrient uptake is affected by the other functions that cells must perform to grow and proliferate, and the balance between such functions is governed by the allocation of the cell proteome to different tasks. It is therefore important to understand how microbial community dynamics is influenced by the proteome allocation of its members, and new insights in this direction might help us make more powerful predictions on how microbial communities assemble and evolve [18, 19].

Scott et al. [20] discovered that, despite the complexity of bacterial metabolism, there are very simple relationships that link the fraction of the proteome allocated for nutrient uptake and protein synthesis to bacterial growth rates in isolation, and that reducing such fraction by forcing cells to express useless proteins reduces their growth rate. Such phenomenological relationships are very powerful because they show that there are simple laws describing how bacterial growth is influenced by proteome allocation and gene expression. These laws have recently been applied in many different contexts [21] and have been shown to be an incredibly effective tool to improve our knowledge of microbial metabolism: they have for example helped explaining the occurrence of overflow metabolism in *Escherichia coli* [22] and improving the predictive power of Flux Balance Analysis [23]. However, the experiments by Scott et al. [21] have been performed with bacterial cultures grown in isolation and in exponential phase, and so it is unclear whether one can use their results to predict the dynamics of a multi-strain community in which multiple strains compete for the same resources in a temporally-variable environment.

In this Letter, we build on Scott et al. [20] and show that one can use the relationship between proteome allocation and bacterial growth rate to predict the population dynamics of a simple community composed of two strains of *E. coli* competing for the same resources in environments that vary temporally between high and low nutrient availability, i.e. between exponential and stationary growth phase. We show that by manipulating

* leonardo.paccianimori@phd.unipd.it

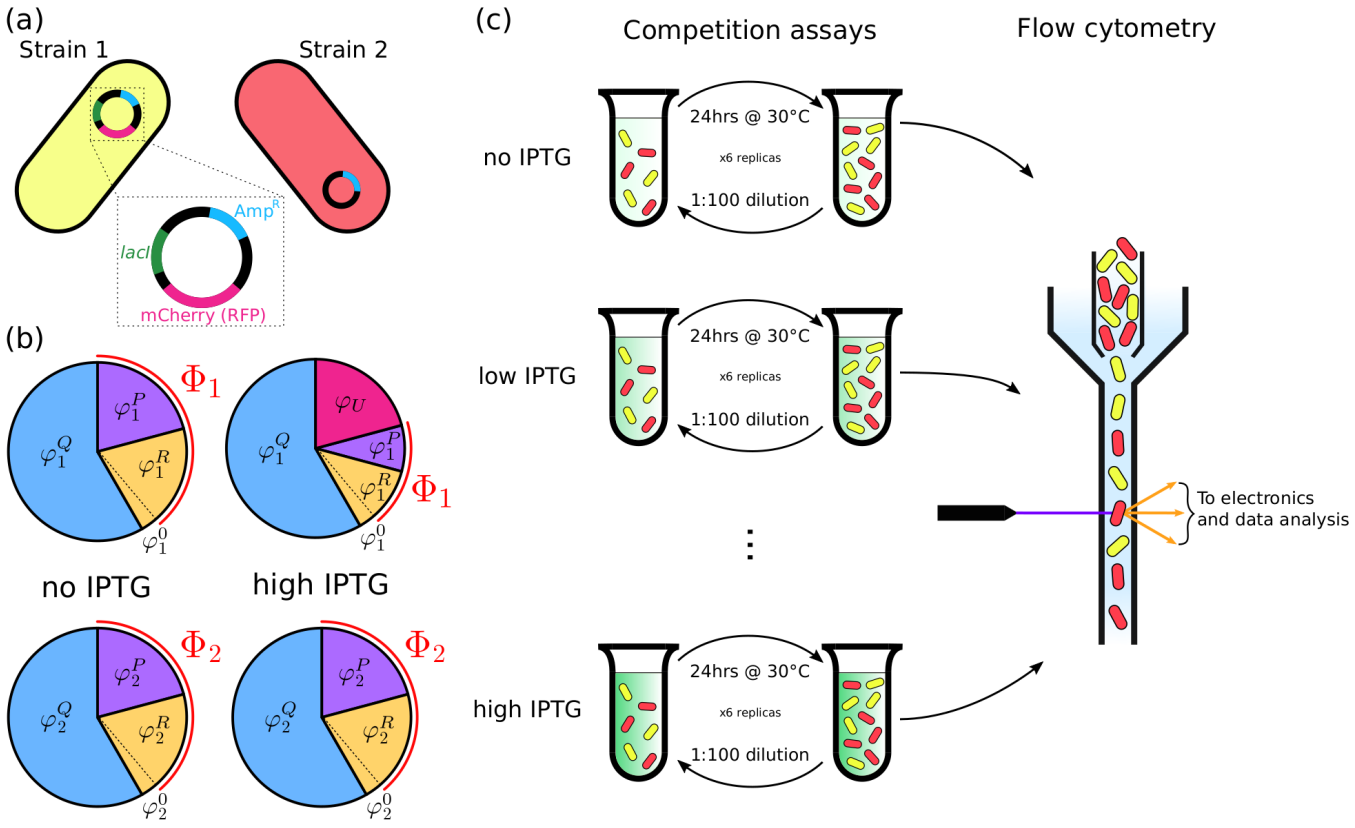

FIG. 1. **(a):** Representation of the strains used for our experiment: strain 1 constitutively expresses a yellow fluorescent protein and carries a plasmid with an ampicillin resistance cassette (cyan gene Amp^R in the plasmid magnification) and a red fluorescent protein, mCherry (magenta gene), under the control of the *trc* promoter (an hybrid of the *trp* and *lac* promoters). The gene *lacI*, also contained in the plasmid, represses the expression of *trc* in the absence of IPTG. On the other hand, strain 2 constitutively expresses a red fluorescent protein and carries a plasmid obtained from the plasmid carried by strain 1, modified so that it only contains the ampicillin resistance cassette. In the Supplemental Material [24] we provide detailed information on the strains used. **(b):** Proteome allocation of the two strains as the concentration of IPTG in the cultures is increased. When strain 1 is cultured in a medium containing IPTG, a fraction φ_U of the strain's proteome is allocated for the expression of the red fluorescent protein mCherry, reducing the fraction Φ_1 allocated for metabolism and growth. On the other hand, when strain 2 is cultured in a medium containing IPTG, its proteome allocation remains unchanged. **(c):** Schematic representation of our experiment. In the Supplemental Material [24] we provide the detailed experimental protocol.

the proteome allocation of one of the two strains, we can control the population dynamics to the point of changing the outcome of competition. We also provide an essential community dynamics model that allows us to make verifiable predictions.

In our experiment, we used two strains of *E. coli* (which we call "strain 1" and "strain 2", Figure 1a) that were engineered so that strain 1 expresses a yellow fluorescent protein (mVenus) constitutively, while strain 2 expresses a red one (mKate2Hyb) constitutively. These fluorescent proteins allowed us to distinguish the two strains at the flow cytometer and measure their relative frequency in the communities (Figure 1c). Furthermore, strain 1 carries a plasmid with a gene encoding for an additional red fluorescent protein (mCherry), whose production can be induced titratably by adding Isopropyl β-D-1-thiogalactopyranoside (IPTG) (a molecular mimic of allolactose that cannot be metabolized by *E. coli*) to the medium. By increasing the concentration of IPTG in the medium, we were thus able to change the overall proteome allocation of the strain, as sketched in Figure 1b, by diverting cellular resources to the production of the protein mCherry. At the start of the experiment, we mixed the two strains in liquid medium, where they competed for nutrients and glucose as the sole common carbon source, at eight different concentrations of IPTG (six technical replicates per IPTG concentration). We re-diluted the cultures daily in fresh medium at a 1:100 ratio for eight days and measured the relative abundances of the two strains at each transfer using flow cytometry. In the Supplemental Material we provide more detailed information on the strains and on the experimental protocol [24].

From a theoretical point of view, the phenomenological framework by Scott et al. [20] prescribes that the proteome of a bacterial strain σ can be minimally divided

into three sectors: a fraction φ_σ^P allocated for nutrient uptake and metabolization, a fraction φ_σ^R allocated for biomass production (i.e., protein synthesis) and a fraction φ_σ^Q allocated for "housekeeping" functions (which they observed to be incompressible); since they are fractions, these three quantities must sum to one:

$$\varphi_\sigma^P + \varphi_\sigma^R + \varphi_\sigma^Q = 1 \ . \tag{1}$$

Given this minimal division of the proteome, Scott et al. [20] have shown that φ_σ^P and φ_σ^R can be written as linear functions of the growth rate g_σ as follows:

$$\varphi_\sigma^P = \frac{\rho_\sigma}{\kappa^n} g_\sigma \ , \tag{2a}$$

$$\varphi_\sigma^R = \frac{\rho_\sigma}{\kappa_\sigma^t} g_\sigma + \varphi_\sigma^0 \ , \tag{2b}$$

where κ^n is the "nutritional capacity" of the (only) energy source used by the strains, κ_σ^t is the "translational capacity" of strain σ (which measures the speed of mRNA translation), ρ_σ is a conversion factor and φ_σ^0 is an "incompressible core" of φ_σ^R. From Eqs (2a) and (2b) we can express φ_σ^R in terms of φ_σ^P, so that Eq (1) can be rewritten as

$$\varphi_\sigma^P \left(1 + \frac{\kappa^n}{\kappa_\sigma^t}\right) = 1 - \varphi_\sigma^Q - \varphi_\sigma^0 := \Phi_\sigma \ , \tag{3}$$

where Φ_σ can be interpreted as the total fraction of species σ's proteome allocated to metabolism and growth.

In our experiment, the two strains started at low density and had enough time to reach saturation before being transferred to fresh medium. As a first approximation, we can write down a minimal model in which the two strains are always growing in the exponential phase, i.e. $\dot{m}_\sigma = m_\sigma \eta_\sigma \varphi_\sigma$, where m_σ is the biomass of species σ, $\eta_\sigma = \kappa^n/\rho_\sigma$ and we write φ_σ instead of φ_σ^P. Eq (3) can be rewritten as $\varphi_\sigma(1+\gamma_\sigma) = \Phi_\sigma$ with $\gamma_\sigma = \kappa^n/\kappa_\sigma^t$. In this approximation, we are not taking into account that cultures are diluted at regular intervals and that the common energy source may run out before the next dilution is made. Nevertheless, in the Supplemental Material [24] we show that results are unaltered when these facts are taken into account. We can set $\eta_1 = \eta_2 = \eta$ and $\gamma_1 = \gamma_2 = \gamma$ since these two strains were engineered starting from the same *E. coli* ancestor strain. Simple computations [24] show that the relative abundance $f_1(t)$ of strain $\sigma = 1$ for small t grows linearly in time with rate:

$$\Lambda_1 \equiv \frac{df_1}{dt}(0) = f_1(0) f_2(0) \frac{\eta}{1+\gamma} (\Phi_1 - \Phi_2) \ , \tag{4}$$

and that the rate of growth of $f_2(t)$ is $\Lambda_2 = -\Lambda_1$. The outcome of competition will thus be determined by the sign of $\Phi_1 - \Phi_2$: if $\Phi_1 > \Phi_2$ (i.e., strain 1 allocates a larger fraction of its proteome to metabolism and biomass production than strain 2) then $\Lambda_1 > 0$, $\Lambda_2 < 0$ and therefore strain 1 will outcompete strain 2; the opposite will happen if $\Phi_1 < \Phi_2$. Coexistence between the two strains will be possible only when $\Phi_1 = \Phi_2$. The system thus exhibits two regimes where only one of the two strains will survive, separated by the coexistence point $\Phi_1 = \Phi_2$.

Experimentally, increasing the concentration of IPTG corresponds to lowering Φ_1, because cellular resources are diverted to the production of the fluorescent protein mCherry. Writing $\Phi_1 = \Phi_1^{(0)} - \varphi_U$, where φ_U is the fraction of proteome allocated by strain 1 for the (useless) synthesis of mCherry, the rates Λ_1 and Λ_2 can be written as linear functions of φ_U with slopes and intercepts of equal magnitude but opposite sign, i.e.

$$\Lambda_1 = \ell - \lambda \varphi_U \qquad\qquad \Lambda_2 = -\ell + \lambda \varphi_U \ , \tag{5}$$

where

$$\ell = f_1(0) f_2(0) \frac{\eta}{1+\gamma} (\Phi_1^{(0)} - \Phi_2) \tag{6a}$$

and

$$\lambda = f_1(0) f_2(0) \frac{\eta}{1+\gamma} \ . \tag{6b}$$

Because the relationship between IPTG concentration and the fluorescence intensity of cells due to the production of mCherry is nonlinear [24], we calibrated the IPTG concentration with the fluorescent intensity of the cells in the arbitrary units returned by the flow cytometer, so that we could express Λ_1 and Λ_2 as functions of the latter [24] (and we are assuming that the measured fluorescent intensity of the cells is proportional to the quantity of fluorescent protein expressed by the cells, i.e. to φ_U). As shown in Figure 2, the two experimentally-measured rates Λ_1 and Λ_2 are indeed linear functions of the fluorescence intensity due to the production of mCherry, as predicted by our theoretical framework. Indeed, a linear fit returns slopes and intercepts that are identical in magnitude within the errors. By manipulating the IPTG concentration, we were able to explore the three predicted regimes of the system. In the absence of IPTG and at low concentrations of it, strain 1 outcompeted strain 2 ($\Lambda_1 > 0$). At an IPTG concentration of approximately 30 μM, the two strains coexisted by maintaining a stable relative fraction. At IPTG concentrations larger than 30 μM, strain 1 was outcompeted by strain 2 (i.e., $\Lambda_1 < 0$).

We found that in the absence of IPTG strain 1 had a fitness advantage over strain 2, i.e. the frequency of strain 1 in the community increased over time. In our theoretical framework, such an advantage means that $\Phi_1^{(0)} - \Phi_2 > 0$. Based on our calculations, we can perform an order-of-magnitude estimate of this difference from Eqs (6a) and (6b):

$$\frac{\ell}{\lambda} = \Phi_1^{(0)} - \Phi_2 \equiv \delta\Phi \ . \tag{7}$$

In order to estimate $\delta\Phi$, we can take ℓ from our fits and calculate λ as follows. First, we compute $f_1(0)$ and $f_2(0)$

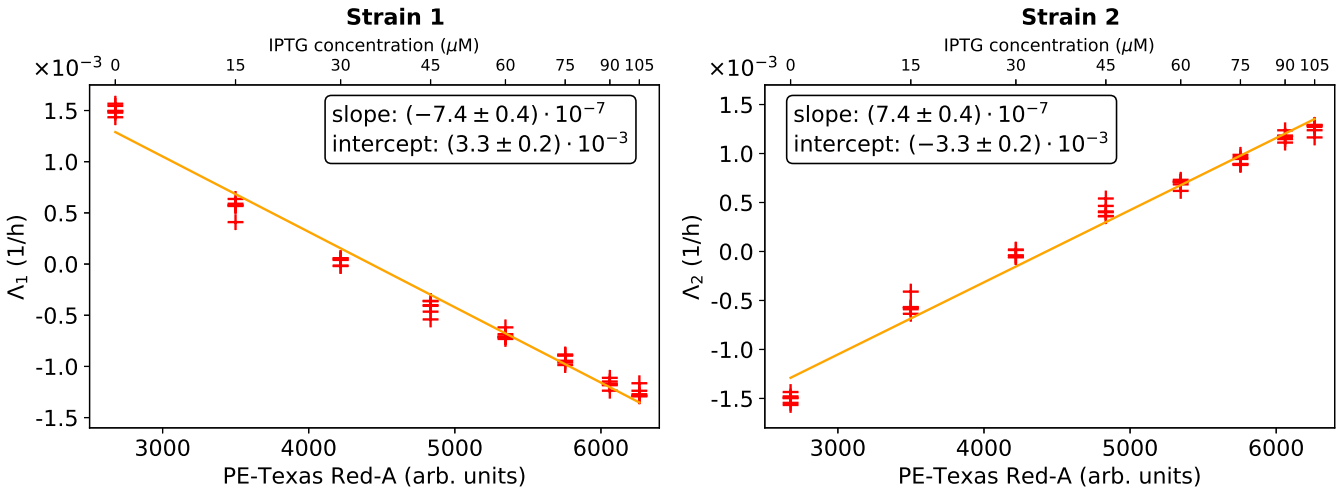

FIG. 2. Results of our experiment. On the horizontal axis is the red fluorescence intensity of the cells (bottom) in the arbitrary units returned by the flow cytometer, and the concentration of IPTG used for the various treatments (top); on the vertical axis is the rate at which the relative abundances of strains 1 (left) and 2 (right) are growing/decreasing. Each red cross in the plots represent one replica for that treatment. In the Supplemental Material [24] we show the time series data of the relative abundances and the conversion between IPTG concentration and fluorescence (arbitrary) units.

from our data as the mean values of the initial conditions for the relative abundances of the two strains. The other parameters, i.e. κ^n, ρ and κ^t, were not measured in our experiment, but we can use the values estimated in [20] for strains with the same genetic background, i.e. strain MG1655 [24]. This indirect estimate limits the accuracy of $\delta\Phi$, but it allows us to evaluate its order of magnitude. With these choices [25], we obtain $\lambda \sim 0.33$ and $\delta\Phi \sim 1\%$.

We have also repeated our experiment with two other strains, strains 3 and 4, that are respectively identical to strains 1 and 2, but with reversed fluorescent protein colors (see Figure S.9): strain 3 constantly expresses a red fluorescent protein and carries a plasmid that allows it to produce a yellow fluorescent protein (Venus YFP) when IPTG is present in the culture medium, and strain 4 constantly expresses a yellow fluorescent protein. All the details of these strains and the results of this second experiment are reported in the Supplemental Material [24]. Despite not being able to span all the regimes exhibited by the system in this case, due to the fact that expressing Venus YFP has a smaller effect on growth rate than expressing mCherry [24], the results are consistent with the ones reported here.

In this Letter we have presented a proof of concept showing how proteome allocation has a central role in shaping and affecting the dynamics of microbial communities. Our experiment shows that changing proteome allocation by inducing the expression of a useless protein, thereby reducing the proteome fraction that cells of one strain allocate to growth and proliferation, has an important effect on the outcome of competition assays and the rate at which a strain increases in frequency in the community and the other one goes extinct. We have also provided a simple community dynamics model capable of explaining our observations. We can thus argue that microbial communities exhibit an additional level of complexity that makes their study even more challenging and intellectually stimulating: in addition to the nontrivial interactions between their constituent parts at the species, strains and individuals level, the properties of such systems will be determined also by how phenomena at both the microscopic (i.e., gene expression and proteome allocation) and macroscopic (i.e. population dynamics) scales influence each other. This work thus provides a first conceptual bridge at the interplay between microbial physiology and community dynamics. In particular, our work constitutes a first step towards the development of the study of microbial competition through population dynamics models grounded on the microscopic properties of microbial communities.

Direct competition for the same common energy source is only one of the many known chemical interactions that can take place in a microbial community [26]: from the exchange of useful metabolites [27, 28] to the production of toxins and antibiotics [29], there are several different ways in which bacteria can allocate their proteome that can have a major impact on community dynamics and structure. This is especially important for engineering synthetic communities in which each member needs to perform a given task, because one needs to balance the production of given a gene product with the growth rate of the strain that produces it, ensuring that the gene product is sufficiently abundant to perform its function and that the strain grows sufficiently fast to persist in the community. Our work shows that these kinds of phenomena must be taken into account in models of community dynamics in order to better understand the fundamental mechanisms that regulate microbial communities.

ACKNOWLEDGMENTS

We thank David R Nelson and Andrew W Murray for hosting L. P.-M. during the experiments. We thank Daniel Eaton for providing the background bacterial strains. A. M. and L. P.-M. acknowledge the Cariparo Foundation for funding. S. S. acknowledges the University of Padua for STARS2018 grants. A. G. was supported by research fellowships from the Swiss National Science Foundation, Projects P2ELP2_168498 and P400PB_180823.

[1] Y. M. Bar-On, R. Phillips, and R. Milo, The biomass distribution on earth, Proceedings of the National Academy of Sciences **115**, 6506 (2018).

[2] D. R. Colman, S. Poudel, B. W. Stamps, E. S. Boyd, and J. R. Spear, The deep, hot biosphere: Twenty-five years of retrospection, Proceedings of the National Academy of Sciences of the United States of America **114**, 6895 (2017).

[3] F. Puente-Sánchez, A. Arce-Rodríguez, M. Oggerin, M. García-Villadangos, M. Moreno-Paz, Y. Blanco, N. Rodríguez, L. Bird, S. A. Lincoln, F. Tornos, O. Prieto-Ballesteros, K. H. Freeman, D. H. Pieper, K. N. Timmis, R. Amils, and V. Parro, Viable cyanobacteria in the deep continental subsurface, Proceedings of the National Academy of Sciences **115**, 10702 (2018).

[4] T. Gold, The deep, hot biosphere, Proceedings of the National Academy of Sciences **89**, 6045 (1992).

[5] I. Sekirov, S. L. Russell, L. C. M. Antunes, and B. B. Finlay, Gut microbiota in health and disease, Physiological Reviews **90**, 859 (2010).

[6] B. K. Singh, R. D. Bardgett, P. Smith, and D. S. Reay, Microorganisms and climate change: terrestrial feedbacks and mitigation options, Nature Reviews Microbiology **8**, 779 (2010).

[7] R. Cavicchioli, W. J. Ripple, K. N. Timmis, F. Azam, L. R. Bakken, M. Baylis, M. J. Behrenfeld, A. Boetius, P. W. Boyd, A. T. Classen, T. W. Crowther, R. Danovaro, C. M. Foreman, J. Huisman, D. A. Hutchins, J. K. Jansson, D. M. Karl, B. Koskella, D. B. Mark Welch, J. B. H. Martiny, M. A. Moran, V. J. Orphan, D. S. Reay, J. V. Remais, V. I. Rich, B. K. Singh, L. Y. Stein, F. J. Stewart, M. B. Sullivan, M. J. H. van Oppen, S. C. Weaver, E. A. Webb, and N. S. Webster, Scientists' warning to humanity: microorganisms and climate change, Nature Reviews Microbiology **17**, 569 (2019).

[8] E. J. Stewart, Growing unculturable bacteria, Journal of Bacteriology **194**, 4151 (2012).

[9] M. Tikhonov and R. Monasson, Collective Phase in Resource Competition in a Highly Diverse Ecosystem, Physical Review Letters **118**, 048103 (2017), 1609.01270.

[10] S. Butler and J. P. O'Dwyer, Stability criteria for complex microbial communities, Nature Communications **9**, 10.1038/s41467-018-05308-z (2018).

[11] S. Landmann and A. Engel, Systems of random linear equations and the phase transition in MacArthur's resource-competition model, Epl **124**, 10.1209/0295-5075/124/18004 (2018).

[12] L. Niehaus, I. Boland, M. Liu, K. Chen, D. Fu, C. Henckel, K. Chaung, S. E. Miranda, S. Dyckman, M. Crum, S. Dedrick, W. Shou, and B. Momeni, Microbial coexistence through chemical-mediated interactions, Nature Communications **10**, 10.1101/358481 (2019).

[13] R. Marsland, W. Cui, J. Goldford, A. Sanchez, K. Korolev, and P. Mehta, Available energy fluxes drive a transition in the diversity, stability, and functional structure of microbial communities, PLoS Computational Biology **15**, 1 (2019).

[14] D. W. Rivett and T. Bell, Abundance determines the functional role of bacterial phylotypes in complex communities, Nature Microbiology **3**, 767 (2018).

[15] T. N. Enke, M. S. Datta, J. Schwartzman, N. Cermak, D. Schmitz, J. Barrere, A. Pascual-García, and O. X. Cordero, Modular Assembly of Polysaccharide-Degrading Marine Microbial Communities, Current Biology , 1 (2019).

[16] A. Zelezniak, S. Andrejev, O. Ponomarova, D. R. Mende, P. Bork, and K. R. Patil, Metabolic dependencies drive species co-occurrence in diverse microbial communities, Proceedings of the National Academy of Sciences **112**, 201522642 (2015).

[17] S. Louca, S. M. S. Jacques, A. P. F. Pires, J. S. Leal, D. S. Srivastava, L. W. Parfrey, V. F. Farjalla, and M. Doebeli, High taxonomic variability despite stable functional structure across microbial communities, Nature Ecology & Evolution **1**, 0015 (2016).

[18] M. Basan, Resource allocation and metabolism: the search for governing principles, Current Opinion in Microbiology **45**, 77 (2018).

[19] D. Bajic and A. Sanchez, The ecology and evolution of microbial metabolic strategies, Current Opinion in Biotechnology **62**, 123 (2020).

[20] M. Scott, C. W. Gunderson, E. M. Mateescu, Z. Zhang, and T. Hwa, Interdependence of cell growth and gene expression, Science **330**, 10.1177/42.6.8189037 (2010).

[21] M. Scott and T. Hwa, Bacterial growth laws and their applications, Current Opinion in Biotechnology **22**, 559 (2011).

[22] M. Basan, S. Hui, H. Okano, Z. Zhang, Y. Shen, J. R. Williamson, and T. Hwa, Overflow metabolism in Escherichia coli results from efficient proteome allocation, Nature **528**, 99 (2015).

[23] M. Mori, T. Hwa, O. C. Martin, A. De Martino, and E. Marinari, Constrained allocation flux balance analysis, PLOS Computational Biology **12**, 1 (2016).

[24] See supplemental material at [url will be inserted by publisher] for details on the bacterial strains and the plasmids used, the experimental protocol, data, details on the model, and the results of the experiment done with strains 3 and 4. (2019).

[25] In particular, we use the following values from [20]: $\kappa^n = 1.32$, $\rho = 0.76$, $\kappa^t = 4.5$. Furthermore, from our data we get that the average values of the initial relative abundances are $\bar{f}_1(0) \sim 0.55$ and $\bar{f}_2(0) \sim 0.45$.

[26] K. Duan, C. D. Sibley, C. J. Davidson, and M. G. Surette, Chemical Interactions between Organisms in Mi-

crobial Communities, Contributions to Microbiology **16**, 1 (2009).

[27] E. C. Seth and M. E. Taga, Nutrient cross-feeding in the microbial world, Frontiers in Microbiology **5**, 1 (2014).

[28] J. E. Goldford, N. Lu, D. Bajić, S. Estrela, M. Tikhonov, A. Sanchez-Gorostiaga, D. Segrè, P. Mehta, and A. Sanchez, Emergent simplicity in microbial community assembly, Science **361**, 469 (2018).

[29] R. E. Lenski and M. A. Riley, Chemical warfare from an ecological perspective, Proceedings of the National Academy of Sciences **99**, 556 (2002).

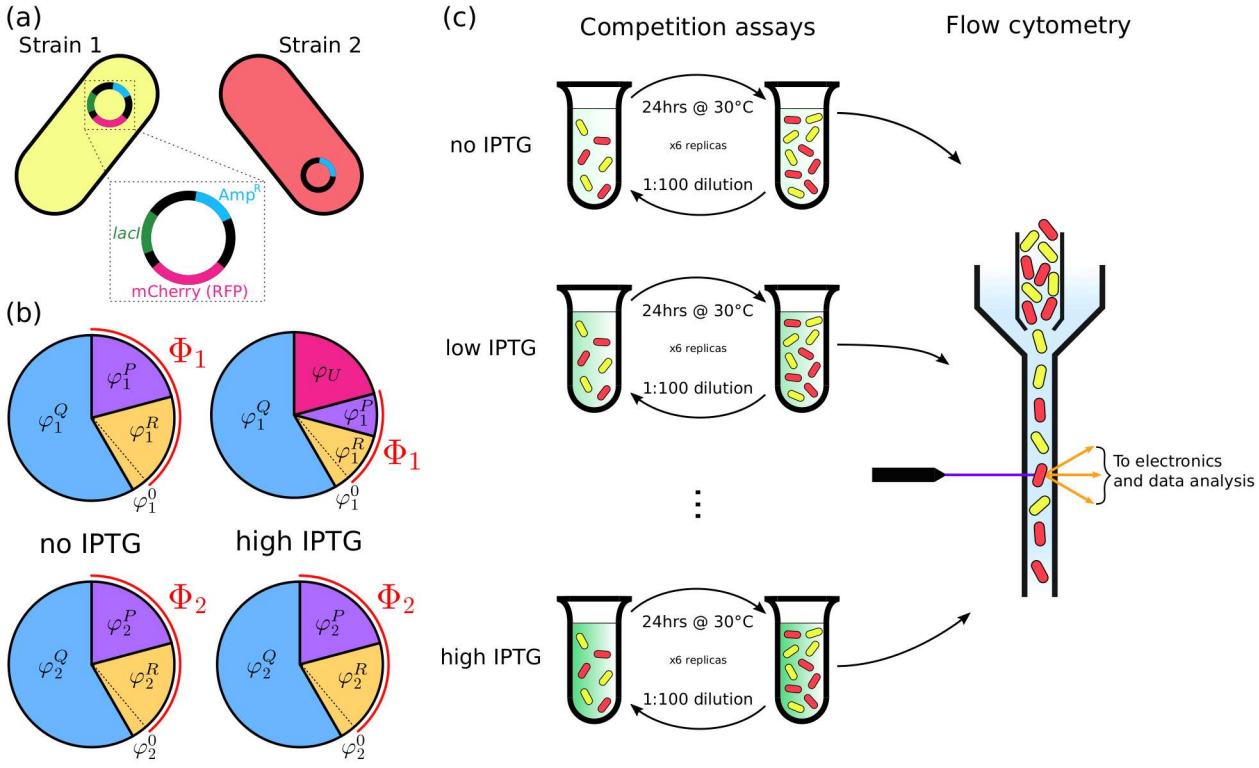
(a)
Strain 1
Strain 2
Amp^R
lacI
mCherry (RFP)
(b)
Φ_1
φ_1^P
φ_1^Q
φ_1^R
φ_1^0
φ_U
no IPTG
high IPTG
Φ_2
φ_2^P
φ_2^Q
φ_2^R
φ_2^0
(c)
Competition assays
Flow cytometry
no IPTG
low IPTG
high IPTG
24hrs @ 30°C
x6 replicas
1:100 dilution
To electronics
and data analysis

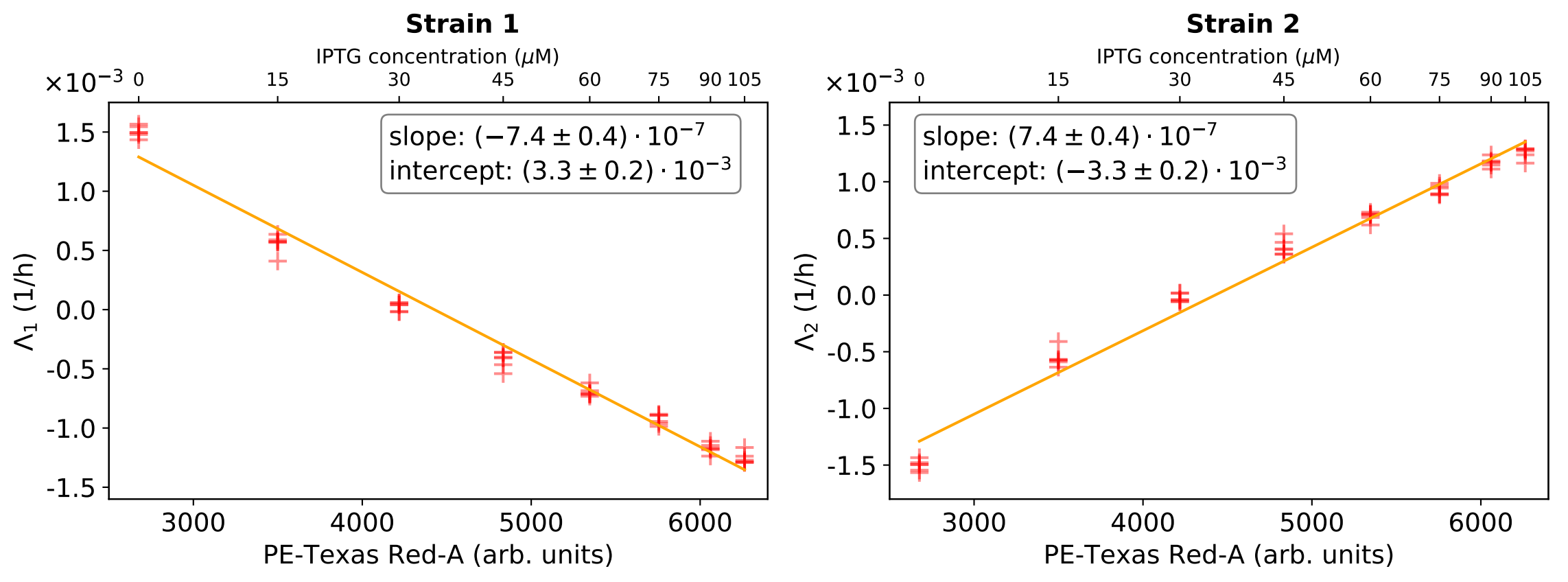
Strain 1
IPTG concentration (μM)
0
15
30
45
60
75
90
105
×10⁻³
1.5
1.0
0.5
0.0
-0.5
-1.0
-1.5
slope: (−7.4 ± 0.4) · 10⁻⁷
intercept: (3.3 ± 0.2) · 10⁻³
Λ1 (1/h)
3000
4000
5000
6000
PE-Texas Red-A (arb. units)
Strain 2
IPTG concentration (μM)
0
15
30
45
60
75
90
105
×10⁻³
1.5
1.0
0.5
0.0
-0.5
-1.0
-1.5
slope: (7.4 ± 0.4) · 10⁻⁷
intercept: (−3.3 ± 0.2) · 10⁻³
Λ2 (1/h)
3000
4000
5000
6000
PE-Texas Red-A (arb. units)